

2016

Recapitulating Cross-Species Transmission of SIVcpz to Humans Using Humanized-BLT Mice

Zhe Yuan

University of Nebraska-Lincoln, s-zyuan1@unl.edu

Guobin Kang

University of Nebraska-Lincoln, gkang2@unl.edu

Fangrui Ma

University of Nebraska-Lincoln, fangrui.ma@gmail.com

Wuxun Lu


University of Nebraska-Lincoln, wlu2@unl.edu

Wenjin Fan

University of Nebraska-Lincoln, wfan3@unl.edu

See next page for additional authors

Follow this and additional works at: <http://digitalcommons.unl.edu/virologypub>

 Part of the [Biological Phenomena, Cell Phenomena, and Immunity Commons](#), [Cell and Developmental Biology Commons](#), [Genetics and Genomics Commons](#), [Infectious Disease Commons](#), [Medical Immunology Commons](#), [Medical Pathology Commons](#), and the [Virology Commons](#)

Yuan, Zhe; Kang, Guobin; Ma, Fangrui; Lu, Wuxun; Fan, Wenjin; Fennessey, Christine M.; Keele, Brandon F.; and Li, Qingsheng, "Recapitulating Cross-Species Transmission of SIVcpz to Humans Using Humanized-BLT Mice" (2016). *Virology Papers*. 310. <http://digitalcommons.unl.edu/virologypub/310>

This Article is brought to you for free and open access by the Virology, Nebraska Center for at DigitalCommons@University of Nebraska - Lincoln. It has been accepted for inclusion in Virology Papers by an authorized administrator of DigitalCommons@University of Nebraska - Lincoln.

Authors

Zhe Yuan, Guobin Kang, Fangrui Ma, Wuxun Lu, Wenjin Fan, Christine M. Fennessey, Brandon F. Keele, and Qingsheng Li

1 Recapitulating Cross-Species Transmission of SIVcpz to Humans Using Humanized-BLT Mice

2

3

4 Zhe Yuan^a, Guobin Kang^a, Fangrui Ma^a, Wuxun Lu^a, Wenjin Fan^a, Christine M. Fennessey^b,

5 Brandon F. Keele^b, Qingsheng Li^{a#}

6

7 Nebraska Center for Virology, School of Biological Sciences, University of Nebraska-Lincoln,

8 Lincoln, NE 68583, USA^a; AIDS and Cancer Virus Program, Leidos Biomedical Research, Inc.

9 Frederick National Laboratory for Cancer Research, Frederick, MD 21702, USA^b

10

11

12 Running Head: Cross-Species Transmission of SIVcpz to Humans

13

14

15 #Address correspondence to Qingsheng Li, qli@unl.edu.

16

17

18 QL and ZY conceived the idea, along with BK designed the experiments; BK provided the virus plasmids;

19 ZY, BK and CF prepared the viral stocks; GK, WL, ZY and WF conducted animal infection and tissue

20 dissection; ZY prepared the *in situ* probes; GK conducted the ISH and IHCS; FM and ZY did the

21 bioinformatics analysis; ZY did all other experiments; ZY and QL wrote the manuscripts.

22

23

24 Abstract: 246 words; Text: 6077 words

25 **ABSTRACT**

26 The origins of HIV-1 have been widely accepted to be the consequence of simian
27 immunodeficiency viruses from wild chimpanzees (SIVcpz) crossing over to humans. However,
28 there has not been any *in vivo* study of SIVcpz infection of humans. Also, it remains largely
29 unknown why only specific SIVcpz strains have achieved cross-species transmission and what
30 transmission risk might exist for those SIVcpz strains that have not been found to infect humans.
31 Closing this knowledge gap is essential for better understanding cross-species transmission and
32 predicting the likelihood of additional cross-species transmissions of SIV into humans. Here we
33 show hu-BLT mice are susceptible to all studied strains of SIVcpz, including the inferred
34 ancestral viruses of pandemic and non-pandemic HIV-1 groups M (SIVcpzMB897) and N
35 (SIVcpzEK505), also strains that have not been found in humans (SIVcpzMT145 and
36 SIVcpzBF1167). Importantly, the ability of SIVcpz to cross the interspecies barrier to infect
37 humanized mice correlates with their phylogenetic distance to pandemic HIV-1. We also
38 identified mutations of SIVcpzMB897 (Env G411R & G413R) and SIVcpzBF1167 (Env H280Q
39 & Q380R) at 14 weeks post inoculation. Together, our results have recapitulated the events of
40 SIVcpz cross-species transmission to humans and identified mutations that occurred during the
41 first 16 weeks of infection, providing *in vivo* experimental evidence that the origins of HIV-1 are
42 the consequence of SIVcpz crossing over to humans. This study also revealed that SIVcpz
43 viruses whose inferred descendants have not been found in humans still have the potential to
44 cause HIV-1 like zoonosis.

45

46

47

48 **IMPORTANCE**

49 It is believed that the origins of HIV-1 are the consequence of SIV viruses from wild
50 chimpanzees crossing over to humans. However, the origins of HIV-1 have been linked back to
51 only specific SIVcpz strains. There have been no experiments that directly test the *in vivo* cross-
52 species transmissibility of SIVcpz strains to humans. This is the first *in vivo* study of SIVcpz
53 cross-species transmission. With the humanized-BLT mouse model, we have provided *in vivo*
54 experimental evidence of multiple SIVcpz strains crossing over to humans and identified several
55 important mutations of divergent SIVcpz strains after long-term replication in human cells. We
56 also found the cross-species transmission barrier of SIVcpz to humans correlates with their
57 phylogenetic distance to pandemic HIV-1 group M. Importantly, this work provides evidence
58 that SIVcpz viruses, whose inferred descendants have not been found in humans, still have the
59 potential to cause a future HIV-1 like zoonotic outbreak.

60

61 **INTRODUCTION**

62 HIV-1 infections have claimed millions of human lives since the pandemic began in 1981 and
63 HIV-1 still infects about 2.3 million people every year (1, 2). Based on comparative phylogenetic
64 analyses of HIV-1 and SIVcpz, it has been shown that AIDS is a zoonotic disease caused by
65 cross-species transmissions of simian immunodeficiency viruses from chimpanzee (SIVcpz) to
66 humans (3, 4). HIV-1 is classified into M, N, O, and P groups and each group is thought to have
67 originated from an independent cross-species transmission. The HIV group M is the causative
68 agent of pandemic HIV/AIDS; in contrast, group N, O, and P viruses only infect a limited
69 number of individuals (5, 6). There are four subspecies of chimpanzees with distinct
70 geographical distribution in Africa: *P. t. verus* in West Africa; *P. t. vellerosus* in Nigeria and
71 northern Cameroon; *P. t. troglodytes* (*Ptt*) in southern Cameroon, Gabon, and the Republic of

72 Congo; and *P. t. schweinfurthii* (*Pts*) in the Democratic Republic of Congo and countries to the
73 East (7). The chimpanzees-*Ptt* and chimpanzees-*Pts* harbor SIVcpz*Ptt* and SIVcpz*Pts*
74 respectively. It has been shown that specific lineages of SIVcpz from the wild chimpanzee
75 subspecies *Ptt* in Africa have founded pandemic HIV-1 group M and non-pandemic group N
76 infections; in contrast, SIVcpz in the wild chimpanzee subspecies *Pts* or other strains from the
77 *Ptt* group have not been found in humans (4-13). However, the reason for this difference is
78 unknown and cannot be explained simply by geographical isolation, because SIVcpzMT145 also
79 belongs to *Ptt* group, but no human infection has been found.

80

81 It is impossible to conduct SIVcpz infection experiments in humans. Moreover, due to the lack
82 of an *in vivo* experimental model, until now there is no investigation on the initial interaction
83 between SIVcpz and humans. Thus, some outstanding questions remain. Can different SIVcpz
84 strains readily infect humans? Why have only specific SIVcpz strains spilled over to humans?
85 For those SIVcpz strains that have not been found in humans, do they still have the potential to
86 cause HIV-like zoonosis? How does SIVcpz adapt in the new human host? However, to date,
87 there is no way to directly study the *in vivo* transmission of divergent strains of SIVcpz to
88 humans.

89

90 The combination of human CD34⁺ pluripotent hematopoietic stem cell transplantation with
91 surgical engraftment of human fetal liver and thymic tissues results in improved immune cell
92 reconstitution, maturation, and selection in humanized bone marrow, thymus, and liver (hu-BLT)
93 mice. This hu-BLT mouse model is the best available animal model for humans (14, 15). Hence,
94 hu-BLT mice provide an ideal *in vivo* model to test the infectivity of different strains of SIVcpz

95 in humans and recapitulate the critical events of SIVcpz cross-species transmission to humans. In
96 addition to the inferred ancestral viruses of HIV-1, chimpanzees or other non-human primates
97 (NHPs) in Africa harbor other viruses which potentially can cause another pandemic zoonotic
98 disease like HIV-1 in the future. Furthermore, there are more than 30 African NHP species that
99 are infected with more than 40 different strains of simian immunodeficiency viruses (SIVs) (16).
100 The conceptual framework and experimental system developed in this study can also be used to
101 evaluate the potential risk of other emerging pathogens from non-human species, especially the
102 great apes, to infect humans by cross-species transmission.

103

104 MATERIALS AND METHODS

105 **Virus stock preparation.** To generate virus, infectious molecular clones of SIVcpz
106 (SIVcpzMB897, SIVcpzMB897-M30R, SIVcpzEK505, SIVcpzEK505-M30R, SIVcpzMT145,
107 and SIVcpzBF1167) and HIV-1_{SUMA} were transfected into 293T cells. Briefly, 60 ug of plasmid
108 DNA diluted into 120ul lipofectamine 2000 (Life Technologies) were used to transfect 293T
109 cells. After 48 hours of transfection, culture supernatant was collected and filtered through a
110 0.45-micron filter from each flask. 35ml of filtered medium was loaded into each Ultra-Clear™
111 Tube (Beckman coulter) for ultracentrifugation. Virus ultracentrifugation was conducted with
112 Optima L-100X ultracentrifuge and SW 32 Ti rotor (Beckman coulter) at 25,000 rpm, 90min at
113 4°C. Supernatant was discarded and the pellet was resuspended into 1ml fresh medium.
114 Aliquoted into 200ul in each sterile screw-cap vial and stored at -150°C. Virus stocks were
115 titrated on the TZM-bl reporter cell line with X-Gal Staining Kit (Genlantis). Titers are
116 expressed as TZM-bl infectious units (IU) per ml.

117

118 **Generation of hu-BLT mice.** Hu-BLT mice generation and assessment of human immune cell
119 reconstitution was conducted as we previously reported (17, 18) at the University of Nebraska-
120 Lincoln Life Sciences Annex according to Institutional Animal Care and Research Committee-
121 approved protocols. Briefly, 6- to 8-week-old female NSG mice (NOD.Cg-Prkdcscid
122 Il2rgtm1Wjl/SzJ, Cat# 005557, the Jackson Laboratory) were housed and maintained in
123 individual micro-isolator cages in a rack system capable of managing air exchange with pre-
124 filters and HEPA filters (0.22 μ m). Room temperature, humidity, and pressure were controlled
125 and air was also filtered. On the day of surgery, mouse received whole-body irradiation at the
126 dose of 12 cGy/gram of body weight with RS200 X-ray irradiator (RAD Source Technologies,
127 Inc., GA) and was then implanted with one piece of thymic tissue fragment sandwiched with two
128 pieces of human fetal liver tissue fragments under the murine left renal capsule. Within 6 hours
129 of surgery, mice were injected via tail vein with $1.5-5 \times 10^5$ CD34⁺ hematopoietic stem cells
130 isolated from human fetal liver tissues. Human fetal liver and thymus tissues were procured from
131 Advanced Bioscience Resources (Alameda, CA). After 9 to 12 weeks, human immune cell
132 reconstitution in peripheral blood was measured by FACS Aria II flow cytometer (BD
133 Biosciences, San Jose, CA) using antibodies against mCD45-APC, hCD45-FITC, hCD3-PE,
134 hCD19-PE/Cy5, hCD4-Alexa 700, and hCD8-APC-Cy7 (Cat#103111, 304006, 300408, 302209,
135 300526, and 301016, respectively, BioLegend, San Diego, CA). Raw data were analyzed with
136 FlowJo (version 10.0, FlowJo LLC, Ashland, OR). All mice used in this study had high human
137 immune reconstitutions with a ratio of hCD45⁺ cells versus a combination of hC45⁺ cells and
138 mCD45⁺ cells in peripheral blood higher than 50% The mice were randomly assigned into
139 experimental groups with similar immune reconstitution levels (Table 1).

140

141 **High-dose SIVcpz infections of hu-BLT mice.** To test human susceptibility to SIVcpz, 25
142 female hu-BLT mice with high immune reconstitution were randomly divided into 5 groups
143 (Table 1) and each mouse was inoculated intraperitoneally (IP) with a high-dose ($3\pm 0.2\times 10^4$ IU)
144 of SIVcpzMB897, SIVcpzEK505, SIVcpzMT145, SIVcpzBF1167, or HIV-1_{SUMA} respectively.
145 Peripheral blood was collected weekly in the first 4 weeks post inoculation (wpi) and once every
146 two weeks thereafter. At 16 wpi, mice were euthanized and the tissues of spleen, lymph node,
147 kidney lymphoid organoid, and jejunum were collected and fixed in 4% paraformaldehyde (PFA)
148 and SafeFix II (Fisher Scientific) for *in situ* tissue analyses. A few hu-BLT mice developed graft-
149 versus-host disease before 16 weeks were sacrificed for humane reason. Fresh tissue was
150 immediately frozen into liquid nitrogen for RNA extraction.

151

152 **Cross-species transmission barrier of SIVcpz.** To quantify the cross-species transmission
153 barrier of SIVcpz to infect humans, each of the SIVcpz strains and HIV-1_{SUMA} was titrated based
154 on viral reverse transcriptase (RT) activity, which is the best available method (19). The RT was
155 measured in triplicate using the EnzChek Reverse Transcriptase Assay Kit (Invitrogen, Eugene,
156 Oregon, USA). The virus strains were lysed using 10% Triton X-100 (1% final concentration) in
157 RPMI medium supplemented with 10% FBS, and HIV-1 Reverse Transcriptase (CHIMERx,
158 Milwaukee, WI, USA) was used as standard curve. Hu-BLT mice with good immune
159 reconstitution were divided into 5 groups (n=6 for SIVcpzMB897 and n=5 for other strains),
160 from which each mouse was inoculated via IP with a low-dose (0.52U/mouse) of SIVcpz or
161 HIV-1_{SUMA}, respectively (Table 1). At 2 and 4 wpi, pVL was measured to determine infection
162 status; If pVL was negative at 4wpi, the animal was considered uninfected and would receive
163 another round of virus inoculation and pVL measurement at 2 and 4 wpi, until all the animals

164 were infected. To determine the interspecies barrier, the Kaplan-Meier plots for conversion to
165 infected status for each SIVcpz group was compared to HIV-1_{SUMA} and Kaplan-Meier plots for
166 conversion to infected status between different SIVcpz strain groups were also compared.

167

168 **Competition of wild-type SIVcpz vs Gag M30R mutant.** To compare the *in vivo* fitness of
169 wild-type SIVcpz and its Gag M30R mutant counterpart, hu-BLT mice (n=6/group) were
170 inoculated with a 1:1 mix of wild-type SIVcpzMB897 or SIVcpzEK505 with its Gag M30R
171 mutant counterpart, respectively. We used inoculum containing both equal copy wild-type and
172 mutant mix (n=3) or equal infectious units of wild-type and mutant mix (n=3), since the latter
173 would eliminate the possibility that equal copy number inoculum may contain an unequal
174 number of infectious viruses. The dose of equal copy mix for each wild-type and mutant was
175 1.53×10^9 for SIVcpzMB897) and 4.1×10^8 for SIVcpzEK505 copies/mouse respectively; and the
176 dose of equal infectious unit mix for SIVcpzMB897 and SIVcpzEK505 was 1.5×10^4 and 1.4×10^4
177 IU/mouse, respectively (Table 1). At 4 wpi, the mice were euthanized and full-length *gag*
178 sequences from plasma were amplified and sequenced using Sanger's method.

179

180 **Plasma viral load.** Plasma viral RNA (vRNA) was extracted using a QIAamp Viral RNA Mini
181 kit (Qiagen). Plasma viral load (pVL) was conducted using qRT-PCR on a C1000 Thermal
182 Cycler and the CFX96 Real-Time system (Bio-Rad) and TaqMan Fast Virus 1-Step Master Mix
183 (Life technologies). SIVcpz strain-specific primers and probes (Table 2) were designed and no
184 crossover signal was found among different strains. The detection limit of pVL was 200
185 copies/ml, which was determined through repeating end point detection of serial dilution of the
186 AcroMetrix HIV-1 Panel (Life technologies).

187

188 ***In situ* hybridization and immunohistochemical staining.** Viral RNA in tissues were detected
189 using *in situ* hybridization (ISH) by following our previously reported protocol (20). To generate
190 sense and anti-sense SIVcpz strain-specific probes, the full-length *gag* and *env* genes of SIVcpz
191 were amplified using RT-PCR with strain specific primers (Table 2). The amplicons were cloned
192 into the pCR[®]4 Blunt-TOPO[®] vector (Thermo Fisher Scientific). Insert orientation was
193 determined by sequencing with T3 and T7 primers at Sequetech (Mountain View, CA) and
194 plasmid DNA was linearized with restriction enzyme Not I or Pme I (New England Biolabs),
195 from which ³⁵S-labeld anti-sense and sense probes were synthesized *in vitro*. Sense probe was
196 used as negative control. After 14 days of exposure, in the developed radioautographs viewed
197 with transmitted light, the vRNA⁺ cells appear black dots; viewed with epipolarized light, the
198 vRNA⁺ cells appear blueish or greenish dots because of the large numbers of silver grains
199 overlying the cell. To define SIVcpz infected cell type, the combined ISH and IHC staining was
200 conducted as previously reported (20). Overnight exposure was used. Anti-CD4 rabbit
201 monoclonal antibody (EPR6855, 1:100 dilution, Abcam) and a cocktail of mouse monoclonal
202 anti-CD68 (KP1, 1:100 dilution, Leica), anti-Ham56 (HAM56, 1:100 dilution, Dako), and anti-
203 CD163(10D6, 1:100, Leica) antibodies were used to identify CD4⁺ T cells and macrophages,
204 respectively. We manually counted about 200 viral RNA⁺ cells to determine the percentage of
205 colocalization of viral RNA with CD4⁺ T cells or macrophages.

206

207 **Sequencing of viral genes.** To assess the *in vivo* adaptations of SIVcpz, vRNA was extracted from
208 plasma with RNeasy Plus Mini Kit (Qiagen) from SIVcpzMB897 and SIVcpzBF1167 infected
209 hu-BLT mice at 14 wpi (n=2 and 3 respectively). The cDNA was synthesized using strain-

210 specific primer (Table 2) and Superscript III reverse transcriptase (Life Technologies). The
211 cDNAs were amplified using Q5 Hot Start High-Fidelity DNA Polymerase (New England
212 Biolabs) with strain- and gene-specific primers (Table 2). The amplicons were confirmed by 1.0%
213 agarose gel stained with ethidium bromide and bands were cut and purified by using the
214 GeneJET gel extraction kit (Thermo Scientific). The amplicons of full-length gag, pol, and env
215 regions for each sample were directly sequenced using Sanger's method at Sequetech (Mountain
216 View, CA) or by next-gen sequencing (Illumina Genome Analyzer IIx) at the University of
217 Nebraska Genomics Core (Lincoln, NE). PCR amplicons of some genes were also cloned into
218 the pCR®4 Blunt-TOPO® vector (Thermo Fisher Scientific) for cloning sequencing at
219 Sequetech (Mountain View, CA). Sequencing primers were designed based on primer walking.
220 The sequences were manually examined peak by peak and assembled individually using
221 Sequencher 5.0 (Gene Codes Corp. Ann Arbor, MI) after the ends of sequences containing
222 ambiguous nucleotides were trimmed. The sequences were confirmed by overlapping identical
223 regions. All the data obtained by bulk, cloning, and next-gen sequencing were analyzed and
224 compared.

225

226 **Bioinformatics analysis.** The phylogenetic tree showing the evolutionary relationship between
227 strains of SIVcpz and HIV-1 in Fig. 1 was made from *pol* sequences of SIVcpz, SIVgor, and
228 HIV-1 group M, N, O, and P. The coordinates of *pol* gene are 3887-4778 on the HIV-1/HXB2
229 genome. The *pol* sequences were aligned using MUSCLE 3.8 to generate multiple sequence
230 alignment in PHYLIP interleaved format(21). The alignment used maximum iteration to get the
231 highest accuracy. Phylogenetic analysis was performed using PHYML 3.0(22), an
232 implementation of the maximum likelihood method. The tree was visualized by FigTree 1.4.2

233 (23). The sequences of *env*, *gag*, and *pol* genes from hu-BLT-mouse samples were processed
234 using an in house developed pipeline to identify the mutation sites that had greater than 5%
235 mutation rate in order to reduce background noise. To exclude random mutations, we used the
236 following criteria to identify significant mutations. The nucleotide changes are nonsynonymous
237 which resulted in the same amino acid change in all sequenced animals of each group.
238 Meanwhile, the average nucleotide substitution must be above 20%. The identified nucleotide
239 changes were converted into amino acid mutations. The corresponding positions for these
240 mutations were mapped to and annotated on HIV-1 GP160 trimer using UCSC Chimera 1.10.2
241 (23). A PDB file 3J5M for the trimer structure was downloaded from the RCSB Protein Data
242 Bank. The sequence logos for these identified Env AA mutations were generated from 55 HIV-1
243 M group and 23 available SIVcpz sequences using WebLogo 2.8.2 (<http://weblogo.berkeley.edu>)
244 (24).

245
246 **Statistics.** Logrank and Gehan-Breslow-Wilcoxon(25) were used to test statistical significance of
247 the Kaplan-Meier plots for conversion to infected status between SIVcpz and HIV-1_{SUMA} group
248 and between different SIVcpz groups. Two-way ANOVA was used to test statistical difference
249 of pVL of SIVcpz and HIV-1_{SUMA} at different time points post inoculation. Both tests were
250 performed by using Graphpad Prism software (Graphpad software, San Diego, CA, USA).
251 $P < 0.05$ was considered significant.

252
253 **Data availability.** All sequencing data have been submitted to NCBI BioSample database under
254 the accession numbers SAMN04569153 to SAMN04569164.

255

256 **RESULTS AND DISCUSSION**

257 **Four SIVcpz strains all infect hu-BLT mice.** We first tested whether divergent strains of
258 SIVcpz can infect hu-BLT mice. We selected 4 phylogenetically divergent SIVcpz strains to
259 represent the inferred ancestral viruses of pandemic HIV-1 group M (SIVcpzMB897) and non-
260 pandemic HIV-1 group N (SIVcpzEK505) (6, 26), as well as SIVcpzMT145 (6) and
261 SIVcpzBF1167 (27) whose viral lineages have not been found in humans (4, 8) . We included
262 HIV-1_{SUMA}, a clade B founder virus derived from an HIV-1 acutely infected individual (28),
263 representing the pandemic HIV-1 group M (HIV-1/M). Hu-BLT mice with high human immune
264 reconstitution were randomly divided into 5 groups (n=5/group, Table 1), from which each hu-
265 BLT mouse was inoculated intraperitoneally (IP) with the dosage of $3 \pm 0.2 \times 10^4$ infectious
266 units/mouse (IU). It has been reported that the simian-to-human cross-species transmissions of
267 SIVcpz in Africa mainly occurred through human contact with infected chimpanzee blood
268 through events such as hunting, bush meat preparation, and bites from infected apes (4, 8, 9), we
269 thus did not inoculate virus through a mucosal route. Peripheral blood was collected weekly in
270 the first 4 weeks post inoculation (wpi) and once every 2 weeks thereafter for a total of 16 weeks.
271 Plasma viral loads (pVL) were quantified using qRT-PCR with strain-specific primers and
272 probes (Table 2). As expected, pVL in HIV-1_{SUMA} infected mice reached a plateau ($\sim 10^6$ copies
273 /ml) from 2 to 16 wpi (Fig. 2E). Strikingly, all four SIVcpz strains can infect and replicate in hu-
274 BLT mice with similar kinetics to HIV-1, regardless of whether they come from chimpanzee *Ptt*
275 or *Pts*, including SIVcpzBF1167 and SIVcpzMT145, whose viral lineages have not been found in
276 humans (Fig. 2A-D). Of note, the timing of reaching the pVL plateau for SIVcpzBF1167 was
277 delayed compared to HIV-1_{SUMA} ($p < 0.01$ at 2 wpi, $p < 0.001$ at 3, 4, 6 wpi) (Fig. 2F).

278

279 Lymph node tissues were collected after euthanasia at 16 wpi. Using *in situ* hybridization (ISH)
280 with ^{35}S labeled strain specific anti-sense probes, we detected viral RNA⁺ cells in these tissues
281 from all hu-BLT mice that were infected with each different SIVcpz strain (Fig. 3A,
282 SIVcpzEK505 infected animal as a representative) as compared with the negative control using
283 sense probes (Fig. 3B). We found that humanized mice are susceptible to all 4 divergent strains
284 of SIVcpz infection *in vivo*, suggesting that SIVcpz strains that have not been found in humans
285 have the ability to infect human cells, which may generate a HIV-1 like zoonosis. SIVcpz
286 infected cell types *in vivo* were determined by using a combination of ISH and
287 immunohistochemical staining (IHC) and we demonstrated that the majority of detectable
288 SIVcpz infection occurs in CD4⁺ T cells for all studied SIVcpz strains (88.64±1.89%, Table 3)
289 (Fig. 3C & D, SIVcpzBF1167 infected animal as a representative, blue arrows), and some of
290 detectable SIVcpz infection occurs in macrophages (12.88±1.91%, Table 3) (Fig. 3E & F). The
291 infected cell types are similar among 4 strains of SIVcpz infected hu-BLT mice, which is
292 consistent with HIV-1 infection in humans (20).

293

294 **The cross-species transmissibility of 4 divergent strains of SIVcpz viruses to humans.**

295 Because SIVcpzMT145 (*Ptt*) and SIVcpzBF1167 (*Pts*) inferred descendant viruses have not
296 been found in humans, our hypothesis is that different SIVcpz strains have diverse cross-species
297 transmissibility to infect humans. We first sought to normalize the inoculum of the 4 SIVcpz
298 strains and HIV-1_{SUMA}. Since a dose based on IU or TCID₅₀ may be biased due to the human-
299 origin indicator cells, we used reverse transcriptase activity to normalize the dose of inoculum
300 (19). We then reduced the inoculation dose to 0.52 RT units, which is significantly lower (9.42
301 fold reduction of IU on average) than the high-dose inoculum we used in initial infections of hu-

302 BLT mice. We inoculated hu-BLT mice with a repeated, low-dose of SIVcpz through the IP
303 route. Hu-BLT mice were divided into 5 groups (n=5 or 6 for each group, Table 1), from which
304 each mouse was inoculated with each respective virus strain. Plasma VL was measured at 2 and
305 4 wpi to determine infection status. If pVL was negative at 4wpi, the animal was considered
306 uninfected and re-inoculated followed by pVL measurement until all animals were demonstrably
307 infected. The Kaplan-Meier plots for conversion to infected status for each SIVcpz group were
308 compared to the HIV-1_{SUMA} group to quantify the barrier of cross-species transmission for each
309 strain. There are significant differences in the number of inoculations needed for infection
310 between SIVcpzMT145 (Fig. 4C) and SIVcpzBF1167 (Fig. 4D) compared with HIV-1_{SUMA}
311 (P=0.0495 and P=0.0027 respectively). Although differences are not significant, SIVcpzMB897
312 (Fig. 4A) and SIVcpzEK505 (Fig. 4B) required a higher number of inoculations than HIV-1_{SUMA}
313 to infect all of the hu-BLT mice (P=0.3613 and P=0.3173 respectively). We then tested the
314 differences between SIVcpz strains in the number of inoculations needed for infection. There are
315 significant differences between SIVcpzMB897 and SIVcpzBF1167 (P=0.0076) as well as
316 between SIVcpzEK505 and SIVcpzBF1167 (P=0.0131); however there are no significant
317 differences between SIVcpzMB897 and SIVcpzEK505 (p=0.9818) or between SIVcpzMT145
318 and SIVcpzBF1167 (p=0.7317). Thus, the cross-species transmission barriers of different
319 SIVcpz strains are correlated with their phylogenetic distance to HIV-1/M (Fig. 1). Our study
320 revealed that the different cross-species transmission barriers of SIVcpz play an important role in
321 determining the establishment and spatial dissemination of pandemic HIV-1. It is also plausible
322 that the different cross-species transmission barriers of SIVcpz may have also impacted the
323 efficiency of initial human-to-human transmission.

324

325 **Mutations of SIVcpz *in vivo*.** It has been proposed that viral adaptation was required to
326 overcome host specific innate restriction factors found between chimpanzees and humans (29-
327 32). To assess the *in vivo* mutations of SIVcpz, we sequenced the major viral genes (*gag*, *pol*,
328 and *env*) at 14 wpi of SIVcpzMB897 and SIVcpzBF1167 in hu-BLT mice. The following criteria
329 were used to identify each significant mutation: nucleotide (nt) changes had to be
330 nonsynonymous, resulting in the same amino acid change for all sequenced animals and the
331 average nt substitution rate from all sequenced animals had to be above 20%. We did not find
332 any cross-animal mutation in *gag* or *pol* that accumulated more than 10% on average at 14 wpi
333 compared with the inoculum. However, as shown in Fig. 5A, next-generation sequencing (NGS)
334 of SIVcpzMB897 *env* gene revealed a consistent G to A change at position 1231 (24.45% on
335 average) and 1237 (53.53% on average) in two sequenced animals as compared with sequences
336 in the inoculum. The detected nt changes correspond to G411R and G413R, respectively. As
337 shown in Fig. 5B, NGS of SIVcpzBF1167 *env* gene revealed a consistent T to A/G change (A/G
338 is synonymous) at position 840 (41.20% on average) and an A to G change at position 1129
339 (58.23% on average) in all three sequenced animals. The detected nt changes correspond to
340 H280Q and Q380R, respectively. We also checked whether the observed SIVcpz mutations exist
341 in HIV-1 Env, as shown in the mutation sequence logos (Fig. 6), we found that all the mutated
342 amino acids exist in HIV-1, three of them are absent in SIVcpz (SIVcpz BF1167 H280Q and
343 Q380R; MB897 G413R). For the SIVcpz BF1167 H280Q mutation, Q is absent in SIVcpz but
344 present in HIV-1 with low frequency. Similarly, for the mutation Q380R, R is absent in SIVcpz
345 but present in HIV-1 with low frequency. For the MB897 G411R mutation, R is present in both
346 SIVcpz and HIV-1; for the MB897 G413R mutation, R is absent in SIVcpz but present in HIV-1.
347

348 Since SIVcpz Env 3D structures are not available, the locations of these mutations were mapped
349 to the corresponding position on the HIV-1 gp160 trimer (Fig. 5C). The G411R, G413R, H280Q,
350 and Q380R mutations were located at the interface between gp41 and gp120, adjacent to or
351 within the CD4 binding loop, respectively (Fig. 5C). The CD4 binding loop of HIV-1 gp120 is
352 essential for interacting with the primary CD4 receptor during viral entry and a site of
353 vulnerability for broadly neutralizing antibodies to target (33, 34).

354

355 Previously, it was reported that all known strains of SIVcpz at position Gag 30 encode a Met (M)
356 or Leu, but many current pandemic HIV-1 strains encode Arg (R) or Lys at that position (35, 36).
357 Moreover, SIVcpz Gag M30R has a fitness advantage over its wild-type counterpart as observed
358 in a replication competition assay using human cells and tonsillar explant cultures (35, 36). Thus,
359 we compared the fitness of Gag M30R mutants of SIVcpzMB897 and SIVcpzEK505 to their
360 wild-type counterparts in an *in vivo* competition study. To eliminate the possibility that equal
361 copy number may have unequal infectious units, an equal infectious units (IU) mixture
362 competition was also conducted, this was not done in previously reported explant tonsil culture
363 studies. Four groups of hu-BLT mice (n=3/group) were used (Table 1) and each mouse was
364 inoculated with an equal copy or equal IU mix of wild type and mutant virus. At 4 wpi, the
365 SIVcpzMB897 M30R mutant virus was dominant in 5 (3 in equal copy group and 2 in equal IU
366 group) of 6 animals (Fig. 6A & 6B). Interestingly, one animal showed the opposite selection
367 (wild-type dominant) after 4 weeks of competition (Fig. 6B). The SIVcpzEK505 M30R mutant
368 was dominant in all 6 mice (Fig. 6C & 6D). From these *in vivo* competition assays, we conclude
369 that the GagM30R mutation confers a fitness advantage over its wild-type counterpart in most

370 cases. However, we did not detect this Gag M30R mutation after 14 weeks of infection in the hu-
371 BLT mice; one plausible explanation is this *de novo* adaptation may need more time.

372

373 A previous report showed that the *vpu* is also important in the evolution of SIVcpz to HIV-1 to
374 antagonize tetherin function (31). Thus, we also sequenced the full-length *vpu* gene of 4 SIVcpz
375 strain infected hu-BLT mice (n=3/group) at 14 wpi using bulk sequencing. The *vpu* sequences of
376 all 12 samples at 14 wpi are identical to the inoculum sequences, which may indicate that the *de*
377 *nov*o generation of this adaptation of *vpu* may also need additional time or the selective pressure
378 that would have led to those substitutions may not be present in hu-BLT mice.

379

380 In short, using the hu-BLT mice model, our results for the first time clearly demonstrate that hu-
381 BLT mice are susceptible to all studied SIVcpz strains *in vivo*, including the inferred ancestral
382 viruses of pandemic and non-pandemic HIV-1 groups M (SIVcpzMB897) and N
383 (SIVcpzEK505), as well as the strains that have not been found in humans (SIVcpzMT145 and
384 SIVcpzBF1167). Importantly, the transmissibility of different SIVcpz strains crossing the
385 interspecies barrier to infect humanized mice is inversely correlated with their phylogenetic
386 distance to pandemic HIV-1. We also identified *in vivo* mutations of SIVcpzMB897 (Env G411R
387 and G413R) and SIVcpzBF1167 (Env H280Q and Q380R) at 14 weeks post inoculation.
388 Together, our results recapitulated the events of SIVcpz cross-species transmission to humans
389 and identified *in vivo* mutations that occurred in the first 16 weeks of infection, providing *in vivo*
390 experimental evidence that the origins of HIV-1 are the consequence of SIVcpz crossing over to
391 humans. This study also revealed that SIVcpz viruses whose lineages have not been found in
392 humans, although with lower cross-species transmissibility, still have the potential to cause HIV-

393 1 like zoonosis. Since wild NHPs, especially our closest relatives the great apes, still harbor
394 many SIV strains, these reservoirs may continue to pose a risk for potential zoonotic outbreak in
395 humans.

396

397 **FUNDING INFORMATION**

398 This project has been funded in part with NIH P30GM103509, NIH R01 DK087625 (QL), and
399 the Start-up funds from the University of Nebraska-Lincoln (QL), with the National Cancer
400 Institute, National Institutes of Health, under Contract No. HHSN261200800001E (BK).

401

402 **ACKNOWLEDGMENTS**

403 The authors thank Lance Daharsh, Dr. Charles Wood, and Dr. John West for their critical
404 reading of the manuscript.

405

406 **REFERENCES**

- 407 1. **Fauci AS, Folkers GK, Dieffenbach CW.** 2013. HIV-AIDS: much accomplished, much to do. *Nat*
408 *Immunol* **14**:1104-1107.
- 409 2. **Faria NR, Rambaut A, Suchard MA, Baele G, Bedford T, Ward MJ, Tatem AJ, Sousa JD,**
410 **Arinaminpathy N, Pépin J, Posada D, Peeters M, Pybus OG, Lemey P.** 2014. The early spread
411 and epidemic ignition of HIV-1 in human populations. *Science* **346**:56-61.
- 412 3. **Paraskevis D, Lemey P, Salemi M, Suchard M, Van De Peer Y, Vandamme AM.** 2003. Analysis of
413 the evolutionary relationships of HIV-1 and SIVcpz sequences using bayesian inference:
414 implications for the origin of HIV-1. *Mol Biol Evol* **20**:1986-1996.
- 415 4. **Sharp PM, Hahn BH.** 2011. Origins of HIV and the AIDS Pandemic. *Cold Spring Harbor*
416 *Perspectives in Medicine* **1**.
- 417 5. **Huet T, Cheynier R, Meyerhans A, Roelants G, Wain-Hobson S.** 1990. Genetic organization of a
418 chimpanzee lentivirus related to HIV-1. *Nature* **345**:356-359.
- 419 6. **Keele BF, Van Heuerswyn F, Li Y, Bailes E, Takehisa J, Santiago ML, Bibollet-Ruche F, Chen Y,**
420 **Wain LV, Liegeois F, Loul S, Ngole EM, Bienvenue Y, Delaporte E, Brookfield JFY, Sharp PM,**
421 **Shaw GM, Peeters M, Hahn BH.** 2006. Chimpanzee Reservoirs of Pandemic and Nonpandemic
422 HIV-1. *Science* **313**:523-526.
- 423 7. **Gao F, Bailes E, Robertson DL, Chen Y, Rodenburg CM, Michael SF, Cummins LB, Arthur LO,**
424 **Peeters M, Shaw GM, Sharp PM, Hahn BH.** 1999. Origin of HIV-1 in the chimpanzee *Pan*
425 *troglodytes troglodytes*. *Nature* **397**:436-441.

- 426 8. **Hahn BH, Shaw GM, De KM, Cock, Sharp PM.** 2000. AIDS as a Zoonosis: Scientific and Public
427 Health Implications. *Science* **287**:607-614.
- 428 9. **Mourez T, Simon F, Plantier J-C.** 2013. Non-M Variants of Human Immunodeficiency Virus Type
429 1. *Clinical Microbiology Reviews* **26**:448-461.
- 430 10. **Santiago ML, Rodenburg CM, Kamenya S, Bibollet-Ruche F, Gao F, Bailes E, Meleth S, Soong SJ,
431 Kilby JM, Moldoveanu Z, Fahey B, Muller MN, Ayouba A, Nerrienet E, McClure HM, Heeney JL,
432 Pusey AE, Collins DA, Boesch C, Wrangham RW, Goodall J, Sharp PM, Shaw GM, Hahn BH.**
433 2002. SIVcpz in wild chimpanzees. *Science* **295**:465.
- 434 11. **Worobey M, Santiago ML, Keele BF, Ndjango J-BN, Joy JB, Labama BL, Dheda BD, Rambaut A,
435 Sharp PM, Shaw GM, HahnBeatrice H.** 2004. Origin of AIDS: Contaminated polio vaccine theory
436 refuted. *Nature* **428**:820-820.
- 437 12. **Sharp PM, Shaw GM, Hahn BH.** 2005. Simian Immunodeficiency Virus Infection of Chimpanzees.
438 *Journal of Virology* **79**:3891-3902.
- 439 13. **Peeters M, Honore C, Huet T, Bedjabaga L, Ossari S, Bussi P, Cooper RW, Delaporte E.** 1989.
440 Isolation and partial characterization of an HIV-related virus occurring naturally in chimpanzees
441 in Gabon. *Aids* **3**:625-630.
- 442 14. **Shultz LD, Brehm MA, Garcia-Martinez JV, Greiner DL.** 2012. Humanized mice for immune
443 system investigation: progress, promise and challenges. *Nat Rev Immunol* **12**:786-798.
- 444 15. **Melkus MW, Estes JD, Padgett-Thomas A, Gatlin J, Denton PW, Othieno FA, Wege AK, Haase
445 AT, Garcia JV.** 2006. Humanized mice mount specific adaptive and innate immune responses to
446 EBV and TSST-1. *Nat Med* **12**:1316-1322.
- 447 16. **VandeWoude S, Apetrei C.** 2006. Going Wild: Lessons from Naturally Occurring T-Lymphotropic
448 Lentiviruses. *Clinical Microbiology Reviews* **19**:728-762.
- 449 17. **Wang L-X, Kang G, Kumar P, Lu W, Li Y, Zhou Y, Li Q, Wood C.** 2014. Humanized-BLT mouse
450 model of Kaposi's sarcoma-associated herpesvirus infection. *Proceedings of the National
451 Academy of Sciences* **111**:3146-3151.
- 452 18. **Li Q, Tso FY, Kang G, Lu W, Li Y, Fan W, Yuan Z, Destache CJ, Wood C.** 2015. Early Initiation of
453 Antiretroviral Therapy Can Functionally Control Productive HIV-1 Infection in Humanized-BLT
454 Mice. *J Acquir Immune Defic Syndr* **69**:519-527.
- 455 19. **Marozsan AJ, Fraundorf E, Abraha A, Baird H, Moore D, Troyer R, Nankja I, Arts EJ.** 2004.
456 Relationships between Infectious Titer, Capsid Protein Levels, and Reverse Transcriptase
457 Activities of Diverse Human Immunodeficiency Virus Type 1 Isolates. *Journal of Virology*
458 **78**:11130-11141.
- 459 20. **Li Q, Duan L, Estes JD, Ma Z-M, Rourke T, Wang Y, Reilly C, Carlis J, Miller CJ, Haase AT.** 2005.
460 Peak SIV replication in resting memory CD4+ T cells depletes gut lamina propria CD4+ T cells.
461 *Nature* **434**:1148-1152.
- 462 21. **Edgar RC.** 2004. MUSCLE: multiple sequence alignment with high accuracy and high throughput.
463 *Nucleic Acids Res* **32**:1792-1797.
- 464 22. **Guindon S, Dufayard JF, Lefort V, Anisimova M, Hordijk W, Gascuel O.** 2010. New algorithms
465 and methods to estimate maximum-likelihood phylogenies: assessing the performance of
466 PhyML 3.0. *Syst Biol* **59**:307-321.
- 467 23. **Pettersen EF, Goddard TD, Huang CC, Couch GS, Greenblatt DM, Meng EC, Ferrin TE.** 2004.
468 UCSF Chimera--a visualization system for exploratory research and analysis. *J Comput Chem*
469 **25**:1605-1612.
- 470 24. **Crooks GE, Hon G, Chandonia JM, Brenner SE.** 2004. WebLogo: a sequence logo generator.
471 *Genome Res* **14**:1188-1190.
- 472 25. **Le CT.** 1997. *Applied survival analysis* New York: John Wiley and Sons

- 473 26. **Heuverswyn FV, Li Y, Bailes E, Neel C, Lafay B, Keele BF, Shaw KS, Takehisa J, Kraus MH, Loul S,**
474 **Butel C, Liegeois F, Yangda B, Sharp PM, Mpoudi-Ngole E, Delaporte E, Hahn BH, Peeters M.**
475 2007. Genetic diversity and phylogeographic clustering of SIVcpzPtt in wild chimpanzees in
476 Cameroon. *Virology* **368**:155-171.
- 477 27. **Li Y, Ndjango J-B, Learn GH, Ramirez MA, Keele BF, Bibollet-Ruche F, Liu W, Easlick JL, Decker**
478 **JM, Rudicell RS, Inogwabini B-I, Ahuka-Mundeke S, Leendertz FH, Reynolds V, Muller MN,**
479 **Chancellor RL, Rundus AS, Simmons N, Worobey M, Shaw GM, Peeters M, Sharp PM, Hahn BH.**
480 2012. Eastern Chimpanzees, but Not Bonobos, Represent a Simian Immunodeficiency Virus
481 Reservoir. *Journal of Virology* **86**:10776-10791.
- 482 28. **Ochsenbauer C, Edmonds TG, Ding H, Keele BF, Decker J, Salazar MG, Salazar-Gonzalez JF,**
483 **Shattock R, Haynes BF, Shaw GM, Hahn BH, Kappes JC.** 2012. Generation of
484 Transmitted/Founder HIV-1 Infectious Molecular Clones and Characterization of Their
485 Replication Capacity in CD4 T Lymphocytes and Monocyte-Derived Macrophages. *Journal of*
486 *Virology* **86**:2715-2728.
- 487 29. **Sauter D, Schindler M, Specht A, Landford WN, Münch J, Kim K-A, Votteler J, Schubert U,**
488 **Bibollet-Ruche F, Keele BF, Takehisa J, Ogando Y, Ochsenbauer C, Kappes JC, Ayouba A,**
489 **Peeters M, Learn GH, Shaw G, Sharp PM, Bieniasz P, Hahn BH, Hatziioannou T, Kirchhoff F.**
490 2009. Tetherin-Driven Adaptation of Vpu and Nef Function and the Evolution of Pandemic and
491 Nonpandemic HIV-1 Strains. *Cell Host & Microbe* **6**:409-421.
- 492 30. **Heeney JL, Dalgleish AG, Weiss RA.** 2006. Origins of HIV and the Evolution of Resistance to AIDS.
493 *Science* **313**:462-466.
- 494 31. **Kirchhoff F.** 2010. Immune Evasion and Counteraction of Restriction Factors by HIV-1 and Other
495 Primate Lentiviruses. *Cell Host & Microbe* **8**:55-67.
- 496 32. **Duggal NK, Emerman M.** 2012. Evolutionary conflicts between viruses and restriction factors
497 shape immunity. *Nat Rev Immunol* **12**:687-695.
- 498 33. **Zhou T, Xu L, Dey B, Hessel AJ, Van Ryk D, Xiang S-H, Yang X, Zhang M-Y, Zwick MB, Arthos J,**
499 **Burton DR, Dimitrov DS, Sodroski J, Wyatt R, Nabel GJ, Kwong PD.** 2007. Structural definition of
500 a conserved neutralization epitope on HIV-1 gp120. *Nature* **445**:732-737.
- 501 34. **Kwong PD, Mascola JR.** 2012. Human antibodies that neutralize HIV-1: identification, structures,
502 and B cell ontogenies. *Immunity* **37**:412-425.
- 503 35. **Wain LV, Bailes E, Bibollet-Ruche F, Decker JM, Keele BF, Van Heuverswyn F, Li Y, Takehisa J,**
504 **Ngole EM, Shaw GM, Peeters M, Hahn BH, Sharp PM.** 2007. Adaptation of HIV-1 to Its Human
505 Host. *Molecular Biology and Evolution* **24**:1853-1860.
- 506 36. **Bibollet-Ruche F, Heigele A, Keele BF, Easlick JL, Decker JM, Takehisa J, Learn G, Sharp PM,**
507 **Hahn BH, Kirchhoff F.** 2012. Efficient SIVcpz replication in human lymphoid tissue requires viral
508 matrix protein adaptation. *The Journal of Clinical Investigation* **122**:1644-1652.

509

510

511

512

513

514 **Figure legends**

515 **FIG 1. The phylogeny of SIVcpz, SIVgor and HIV-1.** The evolutionary relationship of SIVcpz, SIVgor,
516 and HIV-1 group M, N, O, and P is based on *pol* sequences, whose coordinates are 3887-4778 on the
517 HIV-1/HXB2 genome. The viruses used in this study are highlighted in boxes and virus host species are
518 indicated at the right. The scale bar represents 0.06 amino acid replacements per site.

519

520 **FIG 2. SIVcpz pVL kinetics.** Plasma VL over the course up to 16 wpi in 5 groups of hu-BLT mice
521 inoculated with a high-dose of each virus. (A) SIVcpzMB897. (B) SIVcpzEK505. (C) SIVcpzMT145. (D)
522 SIVcpzBF1167. (E) HIV-1_{SUMA}. (F) Plasma VL kinetics of all 5 groups based on the mean values.
523 Dashed line indicates the detection limit of pVL.

524

525 **FIG 3. SIVcpz RNA⁺ cells and infected cell types in lymphoid tissues.** Representative images of
526 lymph node tissues of hu-BLT mice at 16 wpi detected using *in situ* hybridization (ISH) with ³⁵S-labeled
527 probes (A & B) and a combination of ISH and IHC staining (C-F). Viral RNA⁺ cells in SIVcpzEK505
528 infected hu-BLT mouse detected with anti-sense probe (A) or with sense probe as a negative control (B).
529 The majority of viral RNA⁺ cells are colocalized with CD4⁺ T cells (C-D, blue arrows) and some of viral
530 RNA⁺ cells are colocalized with macrophages (E-F) in SIVcpzBF1167 infected hu-BLT mouse. Viral
531 RNA⁺ cells that are not colocalized with macrophages are indicated with red arrows(F).

532

533 **FIG 4. Cross-species transmission barrier of SIVcpz.** Five groups of hu-BLT mice were inoculated
534 with a low-dose of SIVcpz or HIV-1_{SUMA} normalized through RT activity (n=5 or 6). The Kaplan-Meier
535 plots for conversion to infected status for HIV-1_{SUMA} is in red, SIVcpzMB897 in dark blue (A),
536 SIVcpzEK505 in light blue (B), SIVcpzMT145 in dark green (C) and SIVcpzBF1167 in light green (D).
537 P value indicates the significance comparing the two curves, and P<0.05 was considered significant.

538

539 **FIG 5. Env sequencing revealed the mutation of SIVcpz *in vivo* at 14 wpi.** The coverage and depth
540 (square brackets) of next-gen sequencing of SIVcpzMB897 and SIVcpzBF1167 are shown. The expanded
541 images highlight the mutation positions and ratios. A in green, T in red, G in orange and C in blue. (A)
542 SIVcpzMB897 cross-animal mutations at position 1231 & 1237 in hu-BLT mouse 273 and 308. (B)
543 SIVcpzBF1167 cross-animal mutations at position 840 and 1129 in hu-BLT mouse 480, 482 and 483. (C)
544 Amino acid mutations mapped to the corresponding positions on HIV-1 Env trimer. GP120 is in light
545 brown, GP41 is in light grey, the CD4 binding loop in yellow, SIVcpzMB897 G411R & G413R are in
546 purple, SIVcpzBF1167 H280Q is in green and Q380R is in red.

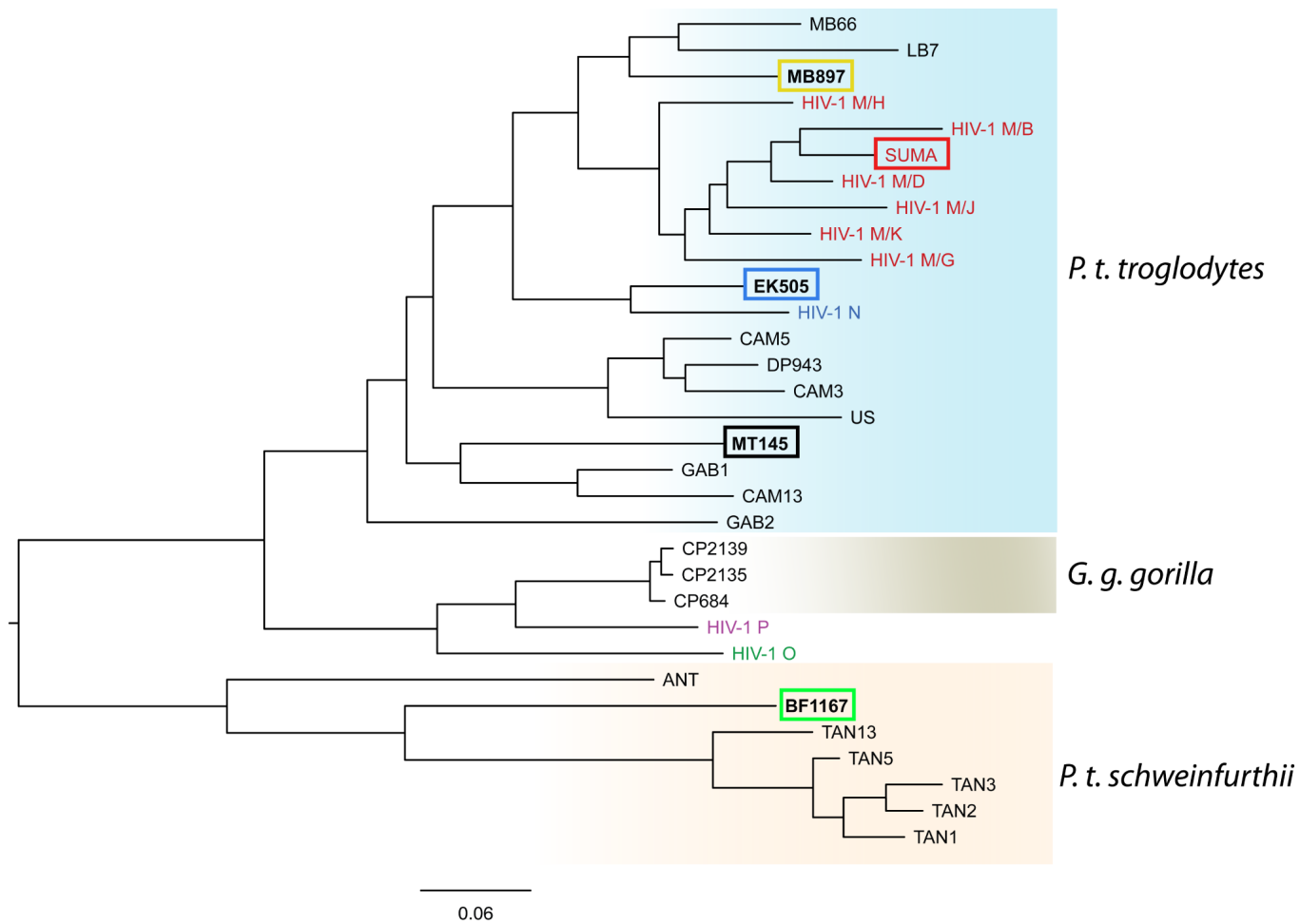
547

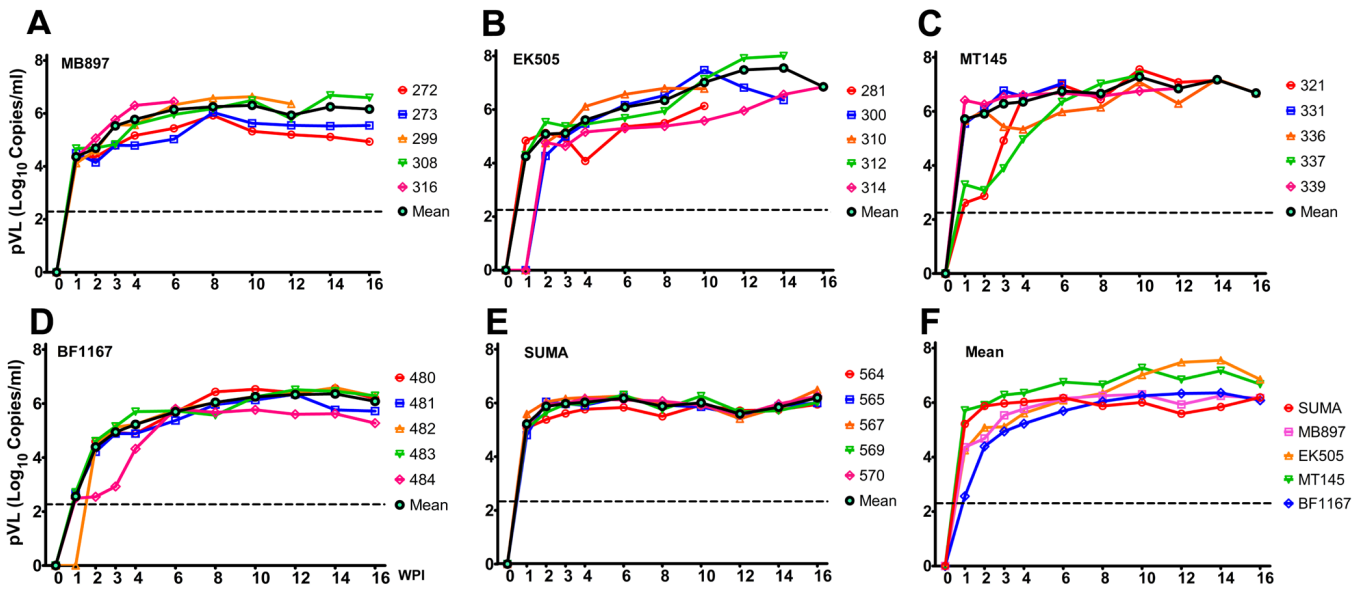
548 **FIG 6. The sequence logos for the identified Env AA mutations.** For the SIVcpz BF1167 H280Q
549 mutation, Q is absent in SIVcpz but present in HIV-1 with low-frequency; similarly for the mutation
550 Q380R, R is absent in SIVcpz but present in HIV-1 with low-frequency. For the MB897 G411R
551 mutation, R is present in both SIVcpz and HIV-1; and for the MB897 G413R mutation, R is absent in
552 SIVcpz but present in HIV-1. Star indicates the original AA in the SIVcpz viruses and arrow indicates
553 mutated AA in HIV-1 at their corresponding positions.

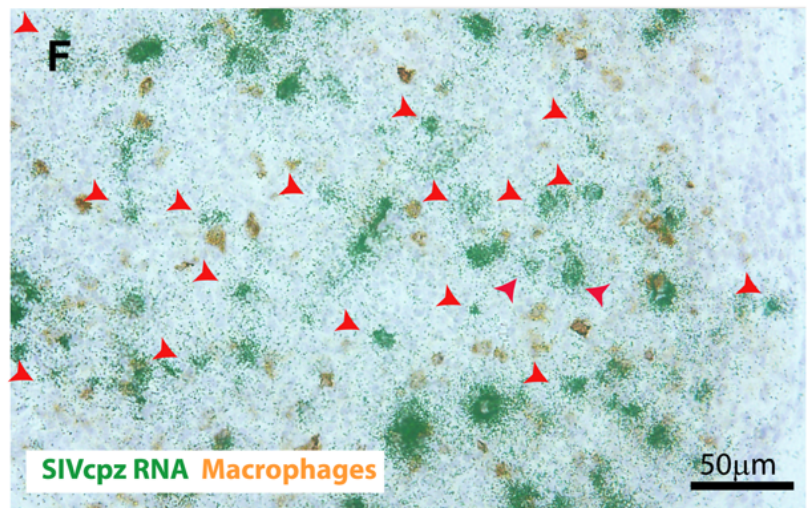
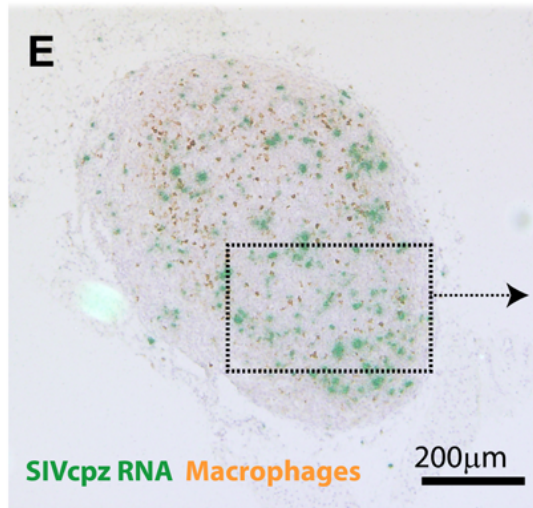
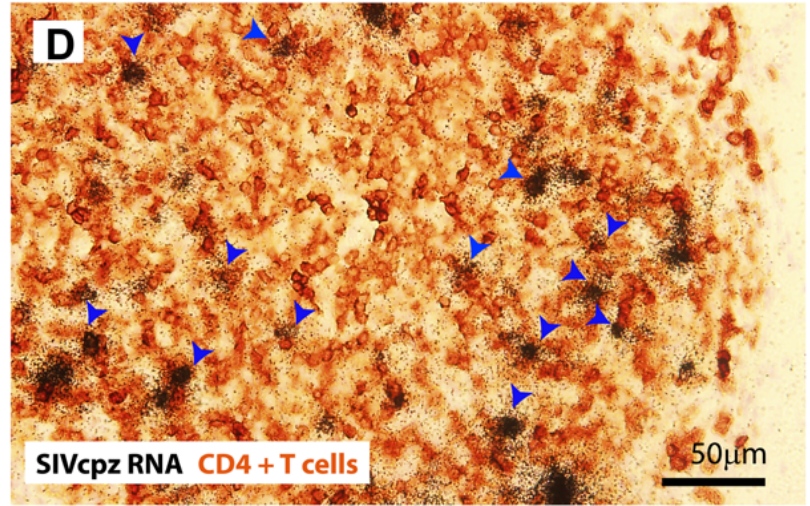
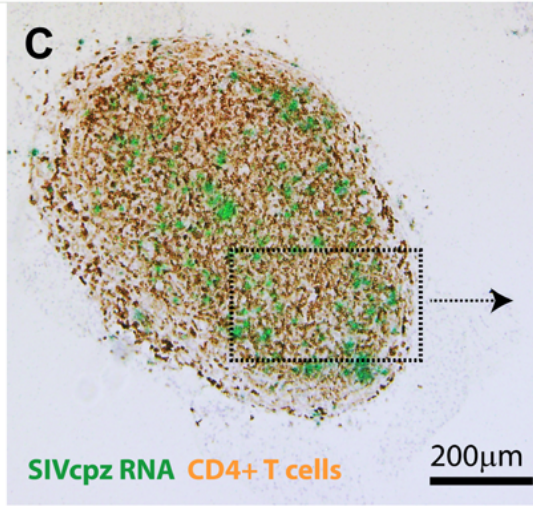
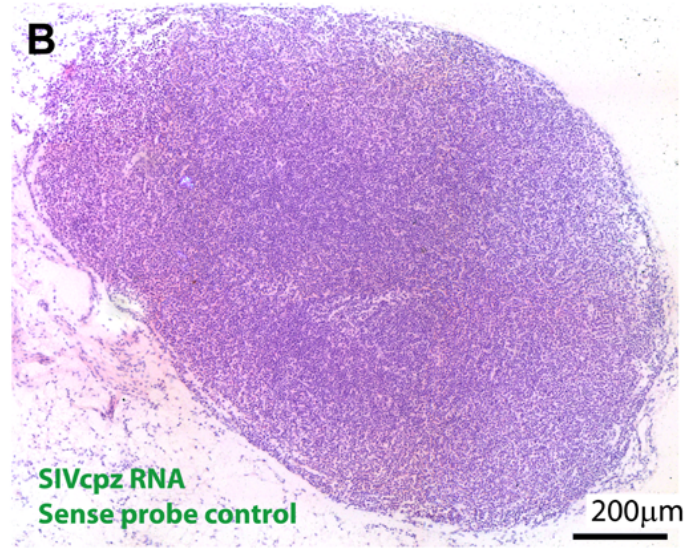
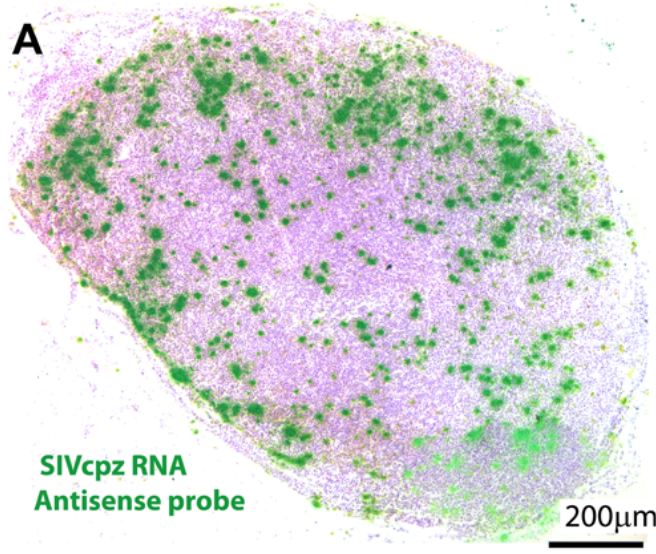
554

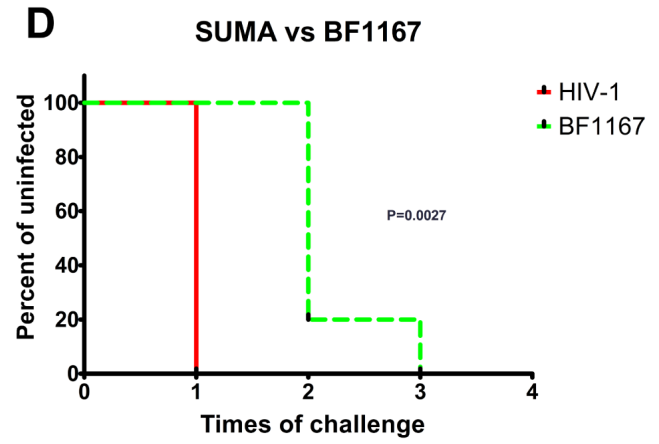
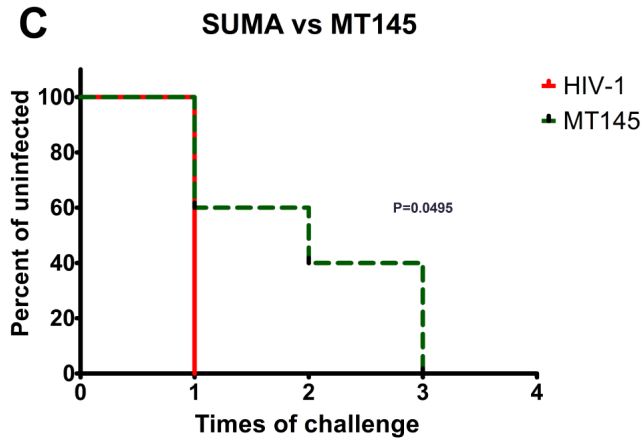
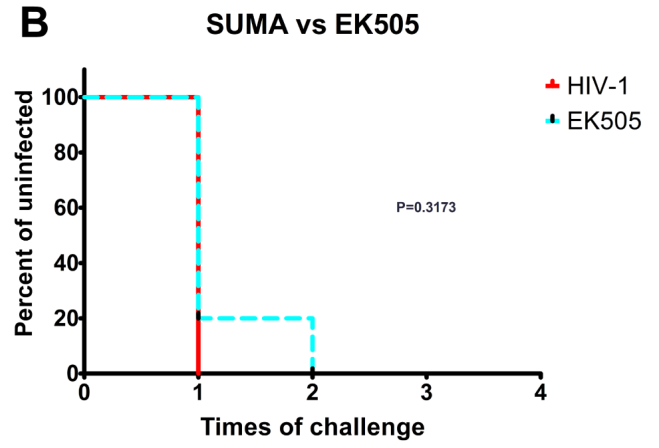
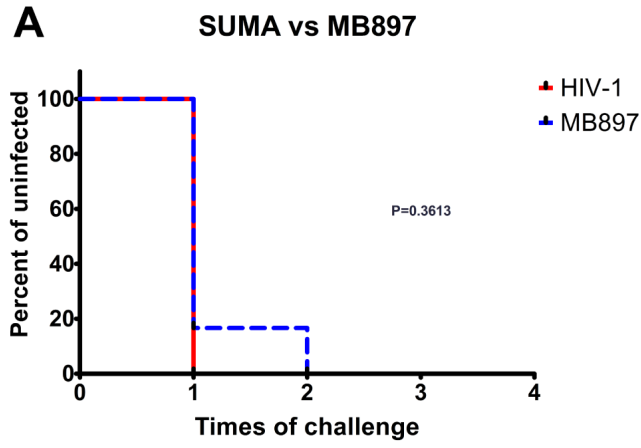
555 **FIG 7. Gag M30R mutant and wide-type *in vivo* competition at 4 wpi.** Red circle indicates the
556 position of Gag 30. (A) SIVcpzMB897 *in vivo* equal copy competition. (B) SIVcpzMB897 *in vivo* equal
557 IU competition. Red line highlighted the only animal with opposite selection. (C) SIVcpzEK505 *in vivo*
558 equal copy competition. (D) SIVcpzEK505 *in vivo* equal IU competition.

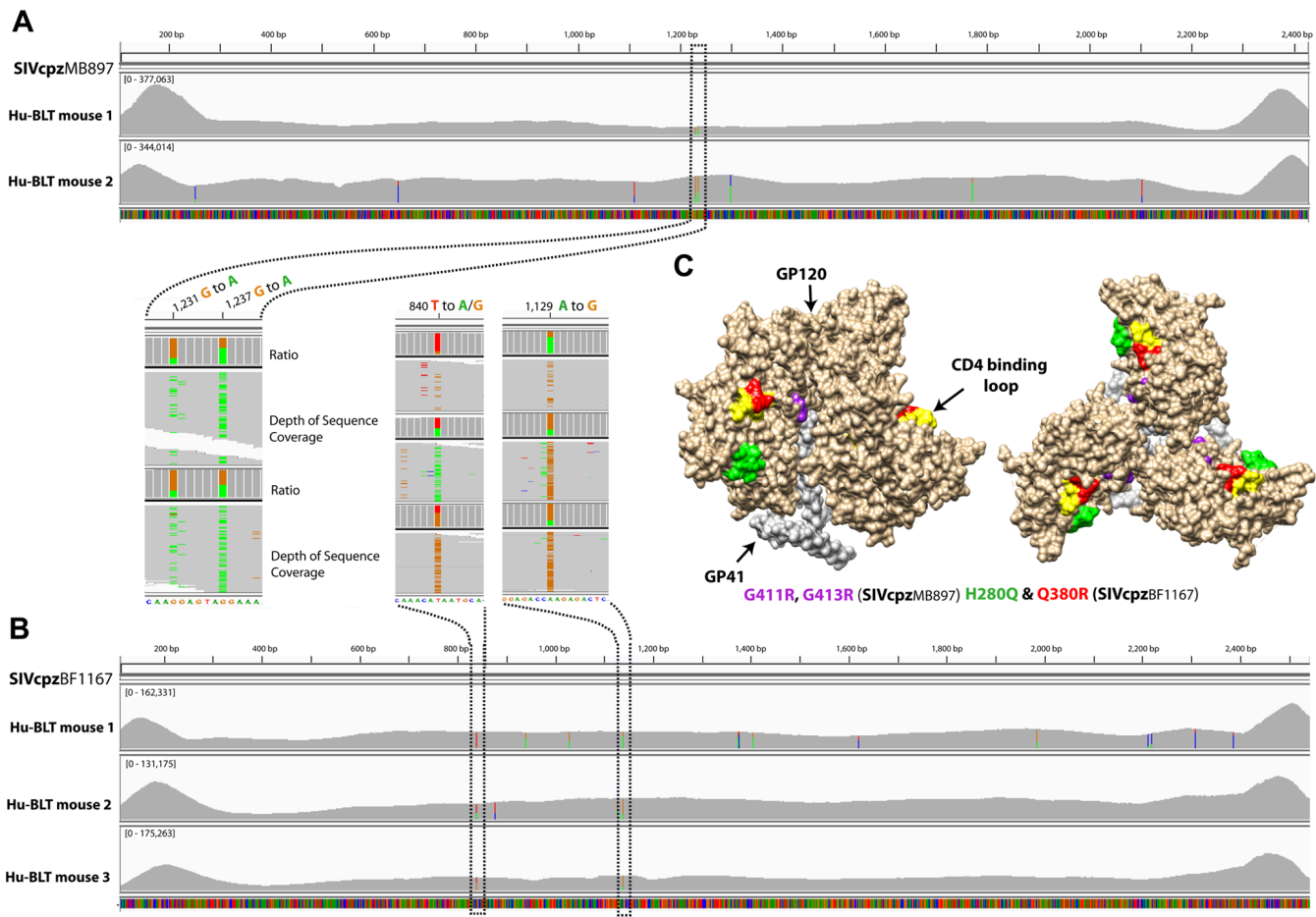
559

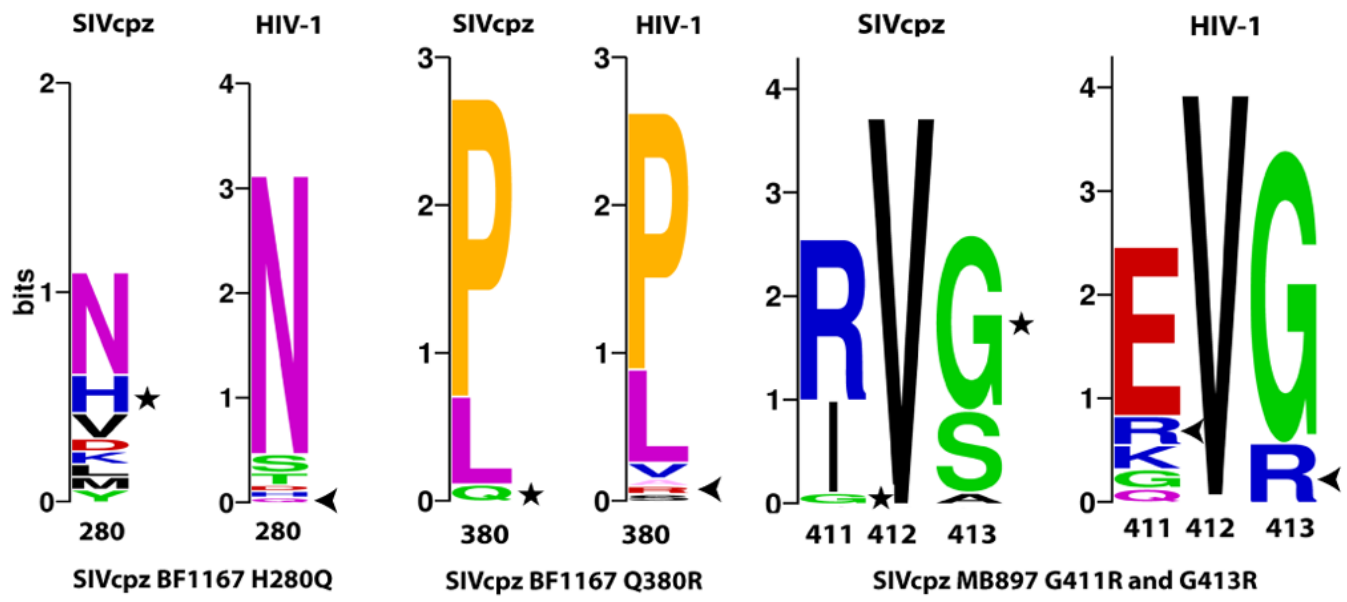












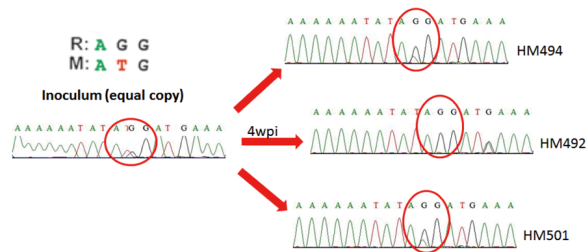
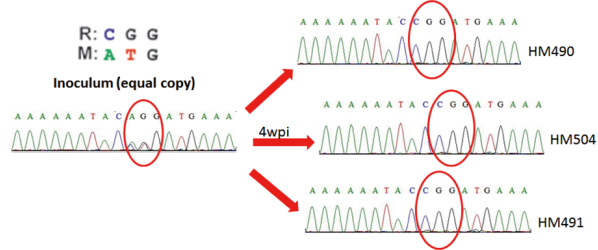
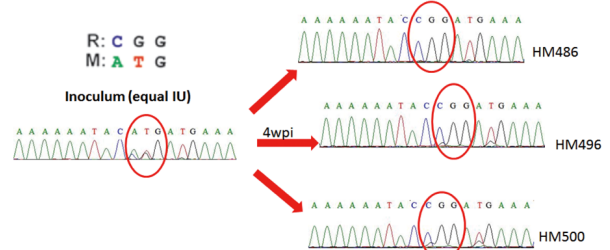
A MB897 *in vivo* Equal Copy Competition**B MB897 *in vivo* Equal IU Competition****C EK505 *in vivo* Equal Copy Competition****D EK505 *in vivo* Equal IU Competition**

Table 1. Hu-BLT Mice Used in the Experiments
High-dose Virus Infectivity Study

Animal ID	% hCD45 ⁺ /(hCD45 ⁺ and mCD45 ⁺ cells)	%hCD3 ⁺ in hCD45 ⁺	%hCD8 ⁺ in hCD45 ⁺ hCD3 ⁺ cells	%hCD4 ⁺ in hCD45 ⁺ hCD3 ⁺ cells	Experiment Group
272*	67.60	82.60	16.40	80.90	MB897
273*	71.70	73.80	17.30	80.40	
299	58.00	48.10	35.80	62.80	
308*	63.50	40.40	22.20	73.50	
316	57.20	30.50	37.70	56.30	
281	85.80	45.10	14.30	82.60	EK505
300*	58.80	52.20	20.30	76.30	
310	65.50	23.40	28.70	64.80	
312*	57.30	25.00	35.10	58.60	
314*	86.80	8.67	37.90	42.20	
321*	87.30	66.80	12.90	83.40	MT145
331	62.60	68.40	12.50	83.90	
336*	68.40	50.70	13.50	82.40	
337	78.40	54.40	14.40	82.30	
339*	64.70	70.00	13.60	81.70	
480*	85.90	49.00	16.40	82.00	BF1167
481	89.20	54.80	15.50	82.70	
482*	80.10	64.40	11.00	85.20	
483*	88.50	57.70	12.80	84.60	
484	84.40	44.70	18.60	79.80	
564	91.70	37.10	21.00	75.70	SUMA
565	86.30	46.80	13.90	84.00	
567	94.30	69.70	14.60	83.30	
569	91.60	36.20	14.80	82.40	
570	93.50	33.30	21.30	75.90	

*indicates the animals whose viral genes have been sequenced.

Low-dose Cross-species Transmission Barrier Study

Animal ID	% hCD45 ⁺ /(hCD45 ⁺ and mCD45 ⁺ cells)	%hCD3 ⁺ in hCD45 ⁺	%hCD8 ⁺ in hCD45 ⁺ hCD3 ⁺ cells	%hCD4 ⁺ in hCD45 ⁺ hCD3 ⁺ cells	Experiment Group
585	94.40	6.84	39.30	55.50	SUMA
587	81.20	30.00	29.90	65.10	
588	92.80	62.90	19.50	77.60	
592	76.80	35.00	28.80	68.60	
593	89.10	49.60	20.30	77.30	
AVG	86.86	36.87	27.56	68.82	
566	80.20	29.40	28.00	69.00	
578	87.90	32.40	19.90	76.80	
584	87.40	9.81	48.40	48.20	
590	84.40	49.20	17.20	80.00	
613	80.80	86.90	10.40	88.80	
619	82.60	66.90	11.10	88.10	
AVG	83.88	45.77	22.50	75.15	
581	88.70	11.50	36.10	58.90	EK505
586	82.40	85.10	13.40	84.90	
589	89.80	28.30	23.30	72.50	
591	94.80	48.80	23.00	73.50	
597	75.80	38.60	15.50	81.20	
AVG	86.30	42.46	22.26	74.20	
530	54.40	36.20	20.20	76.50	
562	79.80	12.90	26.00	69.50	
568	95.80	54.00	13.20	83.20	
574	95.00	47.30	21.60	74.40	
596	82.30	26.80	24.60	72.50	
AVG	81.46	35.44	21.12	75.22	
575	90.60	26.40	18.60	77.70	BF1167
594	78.90	50.50	28.30	68.90	
595	88.00	32.30	15.30	82.40	
598	93.50	45.50	19.40	77.50	
599	79.80	13.10	53.00	41.80	
AVG	86.16	33.56	26.92	69.66	

M30R *in Vivo* Competition Study

Animal ID	% hCD45 ⁺ /(hCD45 ⁺ and mCD45 ⁺ cells)	%hCD3 ⁺ in hCD45 ⁺	%hCD8 ⁺ in hCD45 ⁺ hCD3 ⁺ cells	%hCD4 ⁺ in hCD45 ⁺ hCD3 ⁺ cells	Experiment Group
494	81.10	27.40	12.50	85.00	MB897
492	87.30	42.70	17.00	78.50	
501	86.70	56.80	13.20	84.30	
488	81.20	32.60	14.70	82.90	
487	87.50	45.80	15.60	80.80	
503	91.80	58.30	12.70	84.30	
AVG	85.93	43.93	14.28	82.63	
486	94.30	42.50	12.00	85.30	EK505
496	90.80	58.90	10.70	87.50	
500	90.40	21.90	22.50	73.20	
490	87.30	31.20	10.90	86.30	
491	86.00	33.60	11.90	85.80	
504	86.10	62.70	11.10	87.30	
AVG	89.15	41.80	13.18	84.23	

Table 2. Primers and Probes Used in This Study

Plasma Viral Load			
Virus Strain	Forward	Reverse	Probe
SIVcpzMB897	GCCTCAATAAAGCTTGCCTGAG	GGGCGCCACTGCTAGAGA	/56-FAM/CCAGAGTCA/ZEN/CAAATTGGATGGGCACA/3IABkFQ/
SIVcpzEK505	GCCTCAATAAAGCTTGCCTTGA	GGGCGCCACTGCTAGAGA	/56-FAM/CCAGAGTCA/ZEN/CCGAATGGATGGGCACA/3IABkFQ/
SIVcpzMT145	GCCTCAATAAAGCTTGCCTTGA	GGGCGCCACTGCTAGAGA	/56-FAM/CCAGAGTCA/ZEN/CTGAATAGACGGGCACA/3IABkFQ/
SIVcpzBF1167	CGCTCAATAAAGCTTGCCTGAG	GGGCGCCACTGGTAGAGA	/56-FAM/GCGGAATGA/ZEN/GATGGGCACACACTGAT/3IABkFQ/
HIV-1	GCCTCAATAAAGCTTGCCTTGA	GGGCGCCACTGCTAGAGA	/56-FAM/CCAGAGTCA/ZEN/CACAACAGACGGGCACA/3IABkFQ/
RT Primers			
SIVcpzMB897		AGGCAAGCTTTATTGAGGCTTAAGCAG	
SIVcpzEK505		AGGCAAGCTTTATTGAGGCTTAAGCAG	
SIVcpzMT145		AGGCAAGCTTTATTGAGGCTTAAGCAG	
SIVcpzBF1167		AGGCAAGCTTTATTGAGGCTTAAGCAG	
PCR Primers			
Gag-F		Gag-R	
SIVcpzMB897	ATGGGTGCGAGAGCGTCAGTATTAACGGGAG	CTATTCTTGCTGCGACAACGGGTCGTTGCCA	
SIVcpzBF1167	ATGGGTGCGAGAGCGTCAGTATTGAGGGGAG	TCATTGGTCGCTGCCAAGATGGATTCAGG	
Pol-F		Pol-R	
SIVcpzMB897	TTTTTTAGGGAAAATCTGGCCTCCCGCAA	TTAACTCTCATCCTGTCTATCTGCCAGACAATCATTACC	
SIVcpzBF1167	TTTTTTAGGGAAACGCACCCCTGGTGGG	CTAATCCTCATTCTGTCTATCTGCCACACCACCCGCAC	
Env-F		Env-R	
SIVcpzMB897	ATGAAAGTGATGGGACACAGAGGAGTTGGAAGC	TTATAGCAAAGCTCTTTCTAAACCTTGCTAATTCTTCTAG	
SIVcpzBF1167	ATGAAAATGGCCTTATTAATTGGATGGATCCTGAC	TTAGTTTAGAGCAATTTCTAATCCCTGCCTGATTCTAGTTG	
Vpu-F		Vpu-R	
SIVcpzMB897	ATGGAAATATTCATAATCTT	CTAATAACCCCTAATAGC	
SIVcpzEK505	ATGTTGTTGCTTATAAAG	TCAGACCCAATTATCTT	
SIVcpzMT145	ATGCAGCTAGAAATTG	TCACCAAAACAGGAT	
SIVcpzBF1167	CTGTGGCAATTTTACA	TTACAACAGAAAATAATTGT	

Table 3. SIVcpz Infected Cell Types

SIVcpz	Colocalization of vRNA and CD4 ⁺ Cells (%)	Colocalization of vRNA and macrophages (%)
MB897	88.95	14.29
EK505	89.29	10.07
MT145	90.37	13.85
BF1167	85.96	13.3
Mean ± S.D.	88.64 ± 1.89	12.88 ± 1.91